applied optics

Hybrid wide-band, low-phase-noise scheme for Raman lasers in atom interferometry by integrating an acousto-optic modulator and a feedback loop

Kai Wang,[1,2,3] Zhanwei Yao,[1,2] Runbing Li,[1,2,4] Sibin Lu,[1,2,3] Xi Chen,[1,2] Jin Wang,[1,2,5] and Mingsheng Zhan[1,2,*]

[1]State Key Laboratory of Magnetic Resonance and Atomic and Molecular Physics, Wuhan Institute of Physics and Mathematics, Chinese Academy of Sciences—Wuhan National Laboratory for Optoelectronics, Wuhan 430071, China
[2]Center for Cold Atom Physics, Chinese Academy of Sciences, Wuhan 430071, China
[3]University of Chinese Academy of Sciences, Beijing 100049, China
[4]e-mail: rbli@wipm.ac.cn
[5]e-mail: wangjin@wipm.ac.cn
*Corresponding author: mszhan@wipm.ac.cn

Received 26 October 2015; revised 27 December 2015; accepted 28 December 2015; posted 5 January 2016 (Doc. ID 252685); published 5 February 2016

We report a hybrid scheme for phase-coherent Raman lasers with low phase noise in a wide frequency range. In this scheme, a pair of Raman lasers with a frequency difference of 3.04 GHz is generated by the ±1-order diffracted lights of an acousto-optic modulator (1.52 GHz), where a feedback loop is simultaneously applied for suppressing the phase noise. The beat width of the Raman lasers is narrower than 3 Hz. In the low-frequency range, the phase noise of the Raman lasers is suppressed by 35 dB with the feedback. The phase noise is less than −109 dBc/Hz in the high-frequency range. The sensitivity of an atom gyroscope employing the hybrid Raman lasers can be implicitly improved 10 times. Due to the better high-frequency response, the sensitivity is not limited by the durations of Raman pulses. This work is important for improving the performance of atom-interferometer-based measurements.

OCIS codes: (020.1335) Atom optics; (230.1040) Acousto-optical devices; (140.3550) Lasers, Raman; (140.3518) Lasers, frequency modulated.

http://dx.doi.org/10.1364/AO.55.000989

1. INTRODUCTION

Atom interferometry is a powerful tool for many applications, such as test of the weak equivalence principle [1], measurement of the gravitational constant [2], and realization of gyroscopes [3,4] and gravimeters [5,6]. Raman lasers with a microwave frequency difference play important roles in atom interferometers [7]. The phases of Raman lasers are directly imprinted on the atomic wave packets, and the phase noise limits the sensitivity of an atom interferometer. Usually, the phase of the atom interferometer is determined by the sensitivity function and the phases of Raman lasers [8,9], and the phase noise is accumulated in the whole frequency range. Therefore, Raman lasers with low phase noise in the whole frequency range are important for improving the sensitivities of atom-interferometer-based instruments, such as atom gravimeters and atom gyroscopes.

Two methods are used to produce a Raman-laser pair. One is the optical phase locking loop (OPLL), which locks the phases of two narrow-linewidth lasers [10,11]. The phase noise is suppressed largely in the low-frequency range (<100 kHz). However, in the high-frequency range (>100 kHz), the phase noise is limited by the feedback bandwidth of the electric servo loop [11]. Another method is laser modulation, which can be realized by electro-optic modulators [12,13], current modulation for a vertical-cavity surface-emitting laser [14], or acousto-optic modulators (AOMs) [15–17]. In the modulation method, the phase noise is mainly limited by the performance of the microwave driving signal. In the electro-optic and current modulations, a series of unwanted side bands, which are harmful for atom interferometers, cannot be separated spatially. For example, the AC Stark shifts induced by the redundant side bands may cause systematic errors in the gravity measurement using atom interferometers [18,19]. The unwanted side bands can be spatially separated in the acousto-optic modulation; thus, a pair of clean Raman lasers can be generated and the performance of Raman lasers is very good in the high-frequency range. However, in the low-frequency range, the performance of Raman lasers generated by the AOM is limited by the vibration noise of the independent optical elements.

In this work, we design and implement a hybrid scheme for Raman lasers with low phase noise in a wide frequency range. The Raman lasers are generated by the ±1-order diffracted lights of an AOM, and a feedback loop is used to suppress the phase noise. The linewidths of the Raman lasers are measured by their beat signals, and the spectra of the phase noise with and without the feedback loop are compared. As a result, the phase noise with feedback is suppressed largely in the low-frequency range and it has better performance in the high-frequency range. The sensitivity of an atom gyroscope using the hybrid Raman lasers is discussed.

2. EXPERIMENTAL SETUP

The schematic diagram of the hybrid Raman lasers is shown in Fig. 1. The master laser (ML, New Focus TLB6900) is locked to crossover peaks ($5S_{1/2}, F = 3$ to $5P_{3/2}, F' = 2, 4$ transitions) of ^{85}Rb atoms via saturated absorption spectroscopy. The ML is amplified by a homemade tapered amplifier, and the output power is 300 mW. Then the ML is modulated by a high-frequency AOM (Brimrose, GPF-1500-200-780) [17,20], which is driven by a microwave signal (1.52 GHz). The ±1-order diffracted beams are used as the Raman lasers, and their frequency difference can be tuned in the range of 400 MHz. The diffraction efficiency of the AOM is 20%; thus, we acquire 60 mW for the +1-order diffracted light, but only obtain 30 mW for the −1-order diffracted light due to loss of the reflected beam. Then a feedback loop is applied to suppress the phase noise of the Raman lasers. After the ± 1-order diffracted beams are combined together by a polarized beam splitter (PBS) and two $\lambda/2$ plates, they are converted into the same polarizations by using another PBS and $\lambda/2$ plate. The beat signal (3.04 GHz) of the Raman lasers is detected by a fast photodetector (PD1, New Focus, model 1434); then it is mixed with another microwave signal (2.96 GHz) and the frequency of the beat signal is downconverted to around 80 MHz. After being amplified by a low-noise amplifier (Mini-Circuits ZFL-500LN), the downconverted signal is sent to feedback circuits (Toptica, mFALC 110) that work in the frequency range of 10–200 MHz. The error signal is obtained by comparing the downconverted signal and a reference signal (80 MHz). This error signal is then sent to the frequency control module of the microwave generator to control the driving signal of the AOM. The 80 MHz signal can be used to adjust the frequency difference of the Raman lasers. In order to reduce phase noise, all microwave (signal) generators are synthesized with 10 MHz frequency from a hydrogen clock.

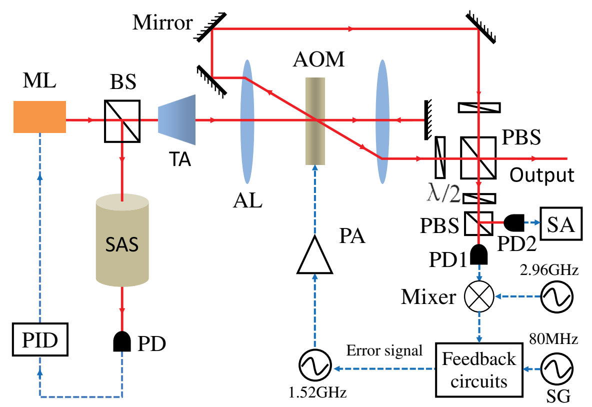

Fig. 1. Schematic diagram of the experimental setup. A pair of Raman lasers is produced by the ±1-order diffracted lights of an AOM, and a feedback loop is applied to suppress the phase noise of the Raman lasers. ML, master laser; SAS, saturated absorption spectroscopy; PID, proportional integral differential circuits; TA, tapered amplified diode laser; AOM, acousto-optic modulator; AL, aspherical lens; BS, beam splitter; PBS, polarized beam splitter; PD, photodetector; PA, power amplifier; SG, signal generator; SA, microwave spectrum analyzer.

3. EXPERIMENTAL RESULTS AND DISCUSSION

After the beat signals are detected by another fast photodetector (PD2, New Focus, model 1434), their linewidths with and without feedback are measured by a microwave spectrum analyzer (Agilent, N9030A). Figure 2 shows the beat signals of 3.04 GHz when the resolution bandwidth (RBW) and the span of the analyzer are set to 1 and 70 Hz, respectively. The black line is the beat signal without feedback, where the measured linewidth is 10 Hz at −80 dBm. The red line is the beat signal with feedback, whose linewidth is less than 3 Hz at −80 dBm [21].

Figure 3 shows the beat signals measured by setting the RBW to 1 Hz but span to 1 kHz. There is serious noise for 100–400 Hz, which is mainly induced by the vibration noise of the optical table [22]. The noise with feedback is suppressed largely by comparing with that without feedback, and the noise suppression ratio is 35 dB at 200 Hz.

In order to characterize the phase noise of the Raman lasers produced by this hybrid scheme, the power spectral density (PSD) is obtained in the whole frequency range (DC–5000 kHz) [23], as shown in Fig. 4. For 10–5000 kHz, the

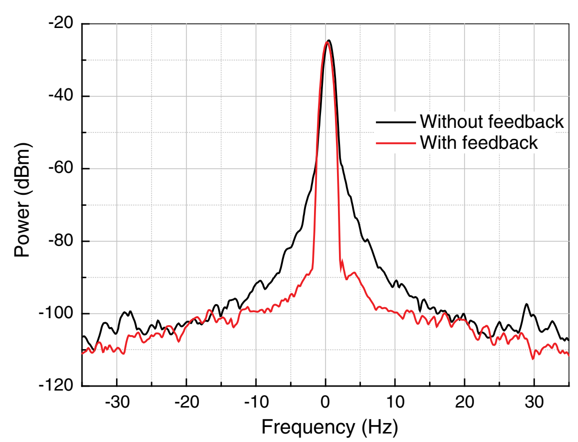

Fig. 2. Beat signals of the Raman lasers measured by setting the RBW of the spectrum analyzer to 1 Hz and span to 70 Hz. The red and black lines are the spectra with and without feedback, respectively.

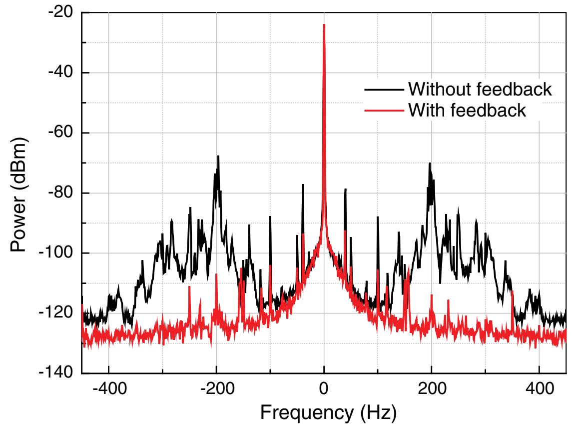

Fig. 3. Beat signals of the Raman lasers measured by setting the RBW of the spectrum analyzer to 1 Hz and span to 1 kHz. The red and black lines are the spectra with and without feedback, respectively.

spectra have outstanding characters, thanks to the lower vibration noise of the optical table [22] where the phase noise with and without feedback are both −109 dBc/Hz. However, the phase noise for 0.1–10 kHz without feedback is bad, and it is only −60 dBc/Hz for 200 Hz (black line). Fortunately, when the hybrid scheme is applied, the phase noise with feedback is suppressed to less than −95 dBc/Hz for 0.1–1 kHz and −105 dBc/Hz for 1–100 kHz (red line). From DC to 100 Hz, the phase noise is close to the phase noise limit of the microwave signal (blue line). There is a small bump at 10 kHz, which is caused by the bandwidth of the feedback circuits.

The hybrid scheme is compared with the OPLL method [10,11] in Table 1 [24]. In the high-frequency range (100–5000 kHz), the phase noise (−109 dBc/Hz) in this hybrid scheme is better than previous best results (−103 dBc/Hz) using the OPLL method [10]. However, in the low-frequency range (DC–100 kHz), the phase noise of the Raman lasers is limited by the performance of the feedback loop. The performance can be improved by using lower noise photodetectors and signal generators. Anyway, in this hybrid scheme, the phase

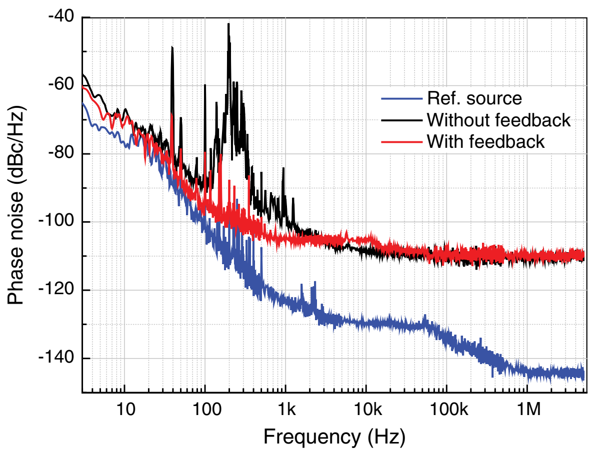

Fig. 4. PSD of the phase noise of the Raman lasers with (red line) and without (black line) feedback in the whole frequency range. The blue line is the PSD of the phase noise of the microwave signal (Agilent, E8257D).

Table 1. Phase Noise of the Raman Lasers in this Work Compared with the OPLL Method [10,11]

Frequency Range (kHz)	OPLL (dBc/Hz)	AOM (dBc/Hz)	Hybrid (dBc/Hz)
0.1–1	−123 [11]	−60	−95
1–10	−130 [11]	−100	−105
10–100	−123 [10]	−108	−105
100–5000	−103 [10]	−109	−109

noise is suppressed largely in the low-frequency range and synchronously held in the high-frequency range.

4. CONTRIBUTION TO AN ATOM GYROSCOPE

We discuss the contribution of such hybrid Raman lasers to the sensitivity of an atom gyroscope when considering the phase noise in the whole frequency range. In an atom interferometer, the phase uncertainty caused by the phase noise of the Raman lasers is given by [10,11]

$$\Delta\Phi^2 = \int_0^\infty S_\varphi(f)|H(2\pi f)|^2 \mathrm{d}f, \tag{1}$$

where $S_\varphi(f)$ is the PSD of the Raman lasers and $|H(2\pi f)|^2$ is the weighting function. The durations of the Raman lasers are usually 1–100 μs [1–7,10,11]. Considering the atom interferometer in which the atomic wave packet is coherently manipulated by three Raman pulses, the weighting function is given by [10,11]

$$|H(\omega)|^2 = \left|\frac{-4\Omega\omega}{\omega^2 - \Omega^2} \sin\left(\omega\frac{T+2\tau}{2}\right) \times \left[\cos\left(\omega\frac{T+2\tau}{2}\right) + \frac{\Omega}{\omega}\sin\left(\omega\frac{T}{2}\right)\right]\right|^2, \tag{2}$$

where τ are the durations of the Raman pulse, T is the time interval between two consecutive Raman pulses, and Ω is the Rabi frequency. Specifically, the rotation sensitivity of the atom gyroscope, in a single measurement, is limited by the phase uncertainty [4]

$$\Delta\Omega_R = \frac{\Delta\Phi}{2k_{\mathrm{eff}} v T^2}, \tag{3}$$

where $\Delta\Omega_R$ is the rotation sensitivity, k_{eff} (for $\lambda = 780$ nm) is the effective wave vector of Raman pulses, and v is the velocity of atoms. Substituting the PSD value in Fig. 4 into Eqs. (1)–(3), we obtain the sensitivity of the atom gyroscope. The sensitivity for $v = 0.6$ m/s, $T = 150$ ms, and $\tau = 100$ μs is plotted in Fig. 5, where $\Delta\Phi$ is obtained against x according to $\Delta\Phi^2 = \int_0^x |H(2\pi f)|^2 S_\varphi(f)\mathrm{d}f$ [25]; then $\Delta\Omega_R$ is plotted from Eq. (3). The black line is the sensitivity of the atom gyroscope without feedback, whereas the red line is that with feedback. This implies that the sensitivity can be improved 10 times due to the lower phase noise in the low-frequency range. Similarly, sensitivities with feedback are also plotted in Fig. 5 (insert), by accumulation for different durations of $T = 50$ ms (black squares), 100 ms (red dots), and 150 ms (blue triangles). The sensitivities are changed by only two times when the durations are decreased from 100 to 1 μs. This is better than the previous results, which are changed 20 times [10] and 100

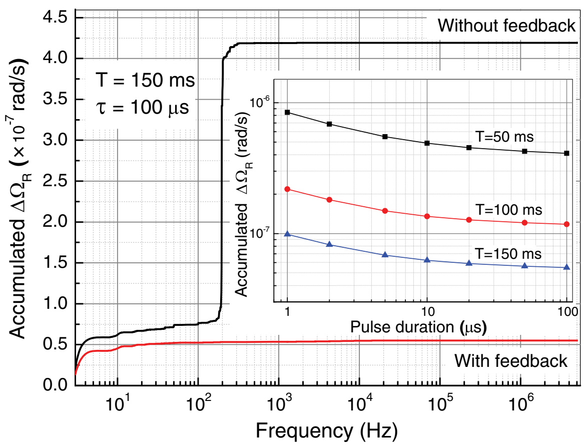

Fig. 5. Sensitivity of an atom gyroscope as a function of the upper limit in the PSD integration, displayed with (red line) and without (black line) feedback for $\tau = 100$ μs, $T = 150$ ms. It is not obviously sensitive to the durations in the hybrid scheme (insert).

times [11] when the durations are decreased from 100 to 1 μs. This indicates that, in this hybrid scheme, the sensitivity is not obviously limited by the durations of the Raman pulses, thanks to their lower phase noise for 10–5000 kHz. To improve the signal-to-noise ratio, shorter Raman pulses are necessary for involving more atoms in the interference process [26], and they can be used to coherently manipulate the states of atoms for improving the performance of atom gyroscopes.

5. CONCLUDING REMARKS

In summary, we have demonstrated a hybrid scheme for low-phase-noise Raman lasers. The phase noise is suppressed largely in the low-frequency range, and its performance is better than that in previous best results in the high-frequency range. The sensitivity of an atom gyroscope with this hybrid scheme can be implicitly improved 10 times. In addition, the sensitivity is not limited by the durations of the Raman pulses. Shorter Raman pulses can be used to coherently manipulate the states of atoms for involving more atoms in the interference process, which is important for improving the performance of atom interferometers.

Funding. National Natural Science Foundation of China (NSFC) (11004227, 91536221).

REFERENCES AND NOTES

1. L. Zhou, S. T. Long, B. Tang, X. Chen, F. Gao, W. C. Peng, W. T. Duan, J. Q. Zhong, Z. Y. Xiong, J. Wang, Y. Z. Zhang, and M. S. Zhan, "Test of equivalence principle at 10^{-8} level by a dual-species double-diffraction Raman atom interferometer," Phys. Rev. Lett. **115**, 013004 (2015).
2. G. Rosi, F. Sorrentino, L. Cacciapuoti, M. Prevedelli, and G. M. Tino, "Precision measurement of the Newtonian gravitational constant using cold atoms," Nature **510**, 518–521 (2014).
3. P. Berg, S. Abend, G. Tackmann, C. Schubert, E. Giese, W. P. Schleich, F. A. Narducci, W. Ertmer, and E. M. Rasel, "Composite-light-pulse technique for high-precision atom interferometry," Phys. Rev. Lett. **114**, 063002 (2015).
4. D. Durfee, Y. Shaham, and M. A. Kasevich, "Long-term stability of an area-reversible atom-interferometer Sagnac gyroscope," Phys. Rev. Lett. **97**, 240801 (2006).
5. A. Peters, K. Y. Chung, and S. Chu, "A measurement of gravitational acceleration by dropping atoms," Nature **400**, 849–852 (1999).
6. Z. K. Hu, B. L. Sun, X. C. Duan, M. K. Zhou, L. L. Chen, S. Zhan, Q. Z. Zhang, and J. Luo, "Demonstration of an ultrahigh-sensitivity atom-interferometry absolute gravimeter," Phys. Rev. A **88**, 043610 (2013).
7. M. A. Kasevich and S. Chu, "Atomic interferometry using stimulated Raman transitions," Phys. Rev. Lett. **67**, 181–184 (1991).
8. P. Cheinet, B. Canuel, F. Pereira Dos Santos, A. Gauguet, F. Leduc, and A. Landragin, "Measurement of the sensitivity function in time-domain atomic interferometer," IEEE Trans. Instrum. Meas. **57**, 1141–1148 (2008).
9. X. Chen, J. Q. Zhong, H. W. Song, L. Zhu, J. Wang, and M. S. Zhan, "Proportional-scanning-phase method to suppress the vibrational noise in nonisotope dual-atom-interferometer-based weak-equivalence-principle-test experiments," Phys. Rev. A **90**, 023609 (2014).
10. M. Schmidt, M. Prevedelli, A. Giorgini, G. M. Tino, and A. Peters, "A portable laser system for high-precision atom interferometry experiments," Appl. Phys. B **102**, 11–18 (2011).
11. S. H. Yim, S. B. Lee, T. Y. Kwon, and S. E. Park, "Optical phase locking of two extended-cavity diode lasers with ultra-low phase noise for atom interferometry," Appl. Phys. B **115**, 491–495 (2014).
12. M. S. Shahriar, A. V. Turukhin, Y. L. Tan, and P. R. Hemmer, "Demonstration of injection locking a diode laser using a filtered electro-optic modulator sideband," Opt. Commun. **184**, 457–462 (2000).
13. H. B. Xue, Y. Y. Feng, X. J. Wang, S. Chen, and Z. Y. Zhou, "Generation of Raman laser beams based on a sideband injection-locking technique using a fiber electro-optical modulator," Rev. Sci. Instrum. **84**, 046104 (2013).
14. W. L. Chen, X. H. Qi, L. Yi, K. Deng, Z. Wang, J. B. Chen, and X. Z. Chen, "Optical phase locking with a large and tunable frequency difference based on a vertical-cavity surface-emitting laser," Opt. Lett. **33**, 357–359 (2008).
15. S. A. DeSavage, K. H. Gordon, E. M. Clifton, J. P. Davis, and F. A. Narducci, "Raman resonances in arbitrary magnetic fields," J. Mod. Opt. **58**, 2028–2035 (2011).
16. P. Bouyer, T. L. Gustavson, K. G. Haritos, and M. A. Kasevich, "Microwave signal generation with optical injection locking," Opt. Lett. **21**, 1502–1504 (1996).
17. P. Wang, R. B. Li, H. Yan, J. Wang, and M. S. Zhan, "Demonstration of a Sagnac-type cold atom interferometer with stimulated Raman transitions," Chin. Phys. Lett. **24**, 536–538 (2007).
18. M. Weitz, B. C. Young, and S. Chu, "Atom manipulation based on delayed laser pulses in three- and four-level systems: light shifts and transfer efficiencies," Phys. Rev. A **50**, 2438–2444 (1994).
19. R. B. Li, L. Zhou, J. Wang, and M. S. Zhan, "Measurement of the quadratic Zeeman shift of ^{85}Rb hyperfine sublevels using stimulated Raman transitions," Opt. Commun. **282**, 1340–1344 (2009).
20. R. B. Li, P. Wang, H. Yan, J. Wang, and M. S. Zhan, "Magnetic field dependence of coherent population transfer by the stimulated Raman transition," Phys. Rev. A **77**, 033425 (2008).
21. The resolution limit of the spectrum analyzer (SA) is 3 Hz, which means it cannot measure signals narrower than 3 Hz.
22. B. Tang, L. Zhou, Z. Y. Xiong, J. Wang, and M. S. Zhan, "A programmable broadband low frequency active vibration isolation system for atom interferometry," Rev. Sci. Instrum. **85**, 093109 (2014).
23. The PSD is calculated after the beat signals are measured by the SA, which is added by 2.27 dBc/Hz due to the equivalent noise bandwidth of the SA and the lower response of the log-averaging of Gaussian noise.
24. In this table, the phase noise in the unit of dBrad^2/Hz in Refs. [10,11] is transformed to the value in the unit of dBc/Hz, and then it is compared with our results.
25. To understand the influence of the phase noise from different frequencies, the phase uncertainty is calculated by the integral from 0 to x, where x is a cut-off frequency when the phase noise is accumulated from 0 to x.
26. For example, the Doppler width is about 30 kHz when the atomic temperate is 5 μK for ^{85}Rb. Thus, the atomic velocity spread is fully covered by the Raman velocity-selective range when the pulse duration is below 5 μs.